FUDMA Journal of Sciences (FJS)
ISSN online: 2616-1370
ISSN print: 2645 - 2944
Vol. 10 No. 8, April, 2026, pp 170 – 182
DOI: https://doi.org/10.33003/fjs-2026-1008-4636

SEQUESTRATION OF Pb^{2+} AND Cd^{2+} IONS FROM AQUEOUS SOLUTIONS USING *Rinorea dentata* LEAF POWDER AS A LOW-COST ADSORBENT

*** [1]Bright Aiyehirue Agwogie, [1]Enebi Estella Jasper, [2]Lanre Tijani Soliu, [3]Evangeline Nwakaego Okotch, [4]Andrew Ogheneovo Onofuevure, [4]Edith Chinyere Unoka, [5]Efetobo Oghenetega and [6]Jamila Bashir Yakasai**

[1]Department of Chemistry, Dennis Osadebay University, Asaba, Delta State, Nigeria.
[2]Department of Chemistry, University of Benin, Benin City, Edo State, Nigeria.
[3]Department of Integrated Science, Federal College of Education (Technical), Asaba, Delta State, Nigeria.
[4]Department of Industrial Chemistry, Dennis Osadebay University, Asaba, Delta State, Nigeria.
[5]Department of Geology, Dennis Osadebay University, Asaba, Delta State, Nigeria.
[6]National Water Resources Institute, Mando, Kaduna State, Nigeria.

* Corresponding authors' email: agwogie.bright@dou.edu.ng

ABSTRACT

Rinorea dentata leaf powder (RDLP) was evaluated as a low-cost adsorbent to sequester Pb^{2+} and Cd^{2+} ions from aqueous solutions. Physicochemical analyses showed a pore volume estimate of 3.8×10^{-3} cm^3/g, low moisture, ash, and volatile matter content. RDLP's surface was confirmed as porous and irregular by scanning electron microscopy, while energy dispersive X-ray spectroscopy (EDX) identified carbon as the dominant element occurring with small amounts of oxygen and nitrogen. Optimal adsorption conditions of 10 mg/L initial metal ion concentration, pH 6, 80 min contact time, 0.6 g adsorbent dose, and 30 µm particle size were determined through batch adsorption experiments conducted at ambient temperature. The Langmuir isotherm model provided a better fit (R^2 = 0.980 for Pb^{2+} and 0.992 for Cd^{2+}) than the Freundlich model, although both models reasonably described the adsorption behaviour, indicating favourable adsorption with predominantly monolayer coverage at lower concentrations, and the presence of surface heterogeneity as suggested by SEM/EDX and the Freundlich model. The pseudo-first order model provided the best fit to the experimental data (R^2 = 0.954 for Pb^{2+} and 0.972 for Cd^{2+}), suggesting physical interactions; however, the intraparticle diffusion contributed to the rate-limiting step, particularly for Cd^{2+} ions. The thermodynamic studies revealed a low enthalpy change (ΔH=14.321 kJ/mol for Pb^{2+} and ΔH =15.026kJ/mol for Cd^{2+} ions, respectively), signifying that the adsorption process was endothermic and thermodynamically feasible with increasing spontaneity at higher temperatures. Overall, RDLP demonstrates strong potential as an inexpensive and effective adsorbent for heavy metal remediation in aqueous systems.

Keywords: Adsorption, Isotherm Models, Metal Ions, *Rinorea dentata*, Thermodynamics

INTRODUCTION

The significant increase in heavy metal concentrations in the environment caused by human activities poses huge risks to public health due to their persistent toxicity and non-biodegradable nature (Saikat *et al.*, 2022) and threatens natural ecosystems. Industrial wastewaters contribute significantly to the release and accumulation of heavy metals in the environment. Metals are known for their wide dispersion in the environment arising from various human and industrial activities such as paper production, metals purification and finishing, manufacturing of chemicals, mining, electroplating, and battery manufacturing. Some metals, such as mercury, lead, cadmium, nickel, and arsenic, have no useful role in human physiology and may be toxic and carcinogenic. Those metals that are considered essential to life, such as iron, copper, magnesium, and zinc, can become harmful at very high levels of exposure (Bayuo*et al*., 2024). Given the toxicological effects of these heavy metals in the environment, animals, and humans, it is imperative to treat industrial wastewater and effluents appropriately before they are discharged into freshwater bodies (Singh *et al*., 2024; Alexander *et al*., 2018).

Different methods, such as precipitation, ion exchange, electro-coagulation, membrane filtration, and packed-bed filtration, have been applied to remove heavy metals from wastewater (Pohl, 2020; Ansam and Sat, 2024; Sohail *et al*.,2020; Khulbe and Matsuura,2018; Shankar *et al*., 2022). Most of these technologies are associated with high operation costs, incomplete metal removal, high energy requirements, and toxic sludge disposal problems (Usman *et al.,* 2024; Abiodun *et al.,* 2023; Anwar *et al.,* 2020). Consequently, these conventional technologies are no longer gaining interest due to low metal ion recovery efficiency and cost implications. Commercial activated carbon is equally cost-prohibitive, especially for large-scale remediation applications (Saleem *et al.*, 2019). In recent years, researchers' interest has shifted to the use of locally available biomass to prepare adsorbents that are cheap and effective. Biosorption offers a feasible, abundant, and economically attractive alternative method for sequestering heavy metals from aqueous solution (Aliyu*et al*., 2026; Xie, 2024; Ekere *et al.*, 2015). The usefulness of biomaterials in removing metal ions from aqueous solution has been investigated, and studies have shown that the plant-based adsorbents have the potential of being used as cheap sources of adsorbent for metal ions removal (Latiza *et al.*, 2024; Subhashish *et al.*, 2023; Jasper *et al.*, 2021; Jain *et al*., 2016; Ekere *et al.*, 2015). Furthermore, the use of raw (unmodified) biomass is advantageous not only due to its low cost but also because it preserves natural surface functional groups such as hydroxyl, carboxyl, and phenolic groups that play a critical role in metal binding, which may be altered or lost during chemical activation processes (Wang *et al*., 2023; He and Chen, 2014).To develop a simple, low-cost biosorbent, this study investigates *Rinorea dentata* leaf powder (RDLP) to remove heavy metals from aqueous solutions.

Rinorea dentata (Kuntze), of the family *Violaceae*, growing in the tropical rainforest regions of Liberia, Cameroon,

Uganda, and Nigeria, is a shrub or small tree up to 10 m high. It is widely distributed in the understory of humid forests, thrives in shaded environments with high moisture content, and regenerates naturally with minimal ecological requirements, making it readily available and sustainable for large-scale applications (Attah *et al*., 2016).It has been reported to be abundant in the rainforest of Omo (Omo Forest Reserve) in Ogun State, South-Western Nigeria, commonly found growing in shady places, occupying the lower story of the dense rainforest (Attah *et al*., 2016). The trunk of the plant provides hardwood; it has a leathery or somewhat coriaceous texture and is locally called *Iyokheze* in Edo and *Oloboroho* in Yoruba, or stone plant. *Rinorea dentata* wood is commonly used as a chewing stick for dental health maintenance, and its phytoextracts have been used in the treatment of malaria (Munvera *et al*., 2020; Attah et al., 2016; Haerdi, 1964). Despite growing interest in plant-based adsorbents, no previous study has systematically evaluated *Rinorea dentata* leaves as a biosorbent for heavy metal removal. This research, therefore, aims to evaluate the potential of the naturally abundant biomass *Rinorea dentata*as a biosorbent for the sequestration of Pb^{2+} and Cd^{2+} ions from aqueous solution. This aim is achieved by applying adsorption isotherm, kinetic, and thermodynamic models to the experimental data to elucidate the adsorption behaviour and its underlying mechanism, and to assess whether untreated RDLP can serve as a viable, low-cost alternative to chemically activated materials.

MATERIALS AND METHODS

Sample Collection and Preparation

Rinorea dentata leaf samples used in this study were obtained from Omo Forest Reserve in Ogun State, Nigeria, and authenticated with voucher number UNN/13091 at the Herbarium domiciled in the Department of Plant Science and Biotechnology, Faculty of Biological Sciences, University of Nigeria, Nsukka. The leaves were washed thoroughly with tap water, rinsed with deionized water to remove dust particles, and then air-dried for 15 days to preserve their surface functional groups and oven-dried afterwards at 105 ^{o}C for 3 h to remove residual moisture. The oven-dried *Rinorea dentata* leaf was ground into powder using a mortar and pestle. The *Rinorea dentata* leaf powder (RDLP) was sieved into various sizes (30, 60, 90,120, 150, and 180 µm) using a rotary sieve shaker (Mashael & Mohammad, 2021). The sieved fractions were stored in different airtight plastic containers before further use to avoid moisture uptake and contamination. No chemical activation, acid treatment, or thermal carbonization was applied to the biomass to evaluate the intrinsic adsorption capacity of the raw material.

Preparation of Pb^{2+} and Cd^{2+} ion Solutions

The reagents used in this study were of analytical grade and were purchased from BDH Laboratories, Germany. The stock solutions of 1000 mg/L of Pb^{2+} and Cd^{2+} ions were prepared by dissolving an appropriate amount of each of Pb $(NO_3)_2$ and $Cd(NO_3)_2.4H_2O$ in double-distilled water. The working solutions were prepared by dilution of the Stock solutions (1000 mg/L) of the individual metal salts, $Pb(NO_3)_2$ and $Cd(NO_3)_2.4H_2O$, with double-distilled water to obtain different metal ion concentrations (10, 20, 30, 40, 50, and 60 mg/L). All glassware was acid-washed (10 % HNO_3) and rinsed with deionized water before use to prevent metal contamination.

Physicochemical Characterization of RDLP

The physicochemical characteristics of RDLP were determined by analyzing for moisture, ash, and volatile matter content according to ASTM Standard methods D7582−15 (Marzeddu *et al*. 2022). Moisture was determined by drying at 105 °C to constant weight; ash was determined by ignition at 550 °C for 3 h in a muffle furnace; and volatile matter was assessed at 900 °C following standard procedures. The method reported by Marzeddu *et al.* (2022) was used to estimate the fixed carbon content, pore volume, porosity, and bulk density of the adsorbent. A digital pH meter and a conductivity meter were used to determine the pH and the conductivity of RDLP. A Scanning Electron Microscope (Phenom World ProX) was used to observe the RDLP surface morphology.

Batch Adsorption Experiments

Adsorption experiments were carried out via batch mode, using 120 mL pre-treated plastic bottles. The studied adsorption parameter values were varied to obtain the optimum conditions. The effect of pH was studied at various pH values ranging from 2 to 12. Following the pH optimization study, the optimum pH obtained was used for all subsequent adsorption experiments. The change in adsorption with respect to initial metal ion concentration was examined at adsorbate concentrations from 10 to 60 mg/L at an optimum pH value of 6. The effect of contact time was determined using a duration range of 20 to 120 minutes. The adsorbent dose was varied from 0.1 to 0.6 g. The particle sizes of RDLP from 30 to 180 µm were investigated. The effect of temperature was examined over a range of 300-350 K using a thermostatic water bath.

For each adsorption experiment, 50 mL of the metal ion solution was measured in the 120 mL plastic bottle. For experiments other than the pH study, the solution pH was adjusted to 6, which was determined as the optimum pH for maximum adsorption efficiency. The adsorbent dosage (0.6 g) and contact time (80 minutes) were maintained at their optimum values except where these parameters were being specifically investigated. The mixture was agitated using a rotary shaker at 180 rpm for 80 minutes. After the equilibrium period of 80 minutes, the solution was filtered using Whatman Grade 42 filter paper, and the residual Pb^{2+} and Cd^{2+} ion concentrations were determined using the Perkin-Elmer AAnalyst 300 Atomic Absorption Spectrometer (AAS). The metal uptake capacity of RDLP biomass and percentage removal of the metal ions was determined using equations 1 and 2.

$$q_e = \frac{(C_o - C_e)V}{M} \quad (1)$$

$$\% \text{ Removal} = 100\left[\frac{C_o - C_e}{C_o}\right] \quad (2)$$

Where q_e = the amount of metal ions adsorbed onto per unit weight of RDLP in mg/g., C_o = Initial metal ion concentration in solution in mg/L.; C_e = Metal ion concentration in the solution at equilibrium in mg/L.; V = Volume of adsorbate in liters; M = Mass of the adsorbent in g. All experiments were performed in triplicate, and average values are reported. Calibration of the AAS was carried out using external standards with correlation coefficients (R^2) exceeding 0.99, and procedural blanks (50 mL of metal ion solution without adsorbent) were prepared and analyzed under identical experimental conditions to account for background contamination and non-adsorptive losses. The concentrations obtained from these blanks were used to correct the final adsorption results. The experimental data were fitted to various equilibrium, isotherm, kinetic, and thermodynamic

parameters to deduce the nature and mechanism of adsorption.

RESULTS AND DISCUSSION

Adsorbent Characterization

RDLP's physicochemical and surface morphological characteristics are presented in Table 1 and Figure 1, respectively, while Table 2 and Figure 2 depict the elemental composition of the RDLP. The adsorbent (RDLP) exhibited percentage values of moisture, ash, and volatile matter, which were low, supporting its suitability as a precursor for an adsorbent (López Pastor *et al*., 2024). The presence of high ash content can block or fill the pores of the adsorbent, reducing its porosity and specific surface area, which are crucial for efficient adsorption. Therefore, low ash value favours the use of biomass as an adsorbent (Zhou *et al*., 2017; Ekere *et al*., 2015).

Table 1: Physicochemical Properties of RDLP

Parameters	Values
Moisture (%)	7.6
Volatile matter (%)	10.3
Ash (%)	4.7
Fixed carbon (%)	77.4
Pore volume (cm^3/g)	3.8×10^{-3}
Bulk density ($g\ mL^{-1}$)	0.34
pH	6.5
Conductivity (µS/cm)	118

The fixed carbon content of RDLP was 77.4%. This value was obtained using the standard proximate analysis relationship (Fixed Carbon = 100 − %Moisture − %Ash − %Volatile Matter), which confirms the internal consistency of the measured parameters (Fajobi *et al*., 2022). However, this value is higher than typically reported for raw biomass materials (Nhuchhen, 2016). This may be attributed to the relatively low combined moisture, ash, and volatile matter contents of the sample, since fixed carbon is calculated by difference. Fixed carbon does not correspond to pure elemental carbon but rather represents the residual fraction remaining after the release of volatile components, and should therefore be interpreted as an indirect measure of carbon content.

The pore volume of 3.8×10^{-3} cm^3/g is modest compared to activated carbons, and it is reasonable for an untreated biomass, indicating that adsorption is likely governed by surface interactions rather than extensive internal pore filling, while high carbon content translates to increased availability of active sorption sites (Kyriakopoulos *et al.,* 2024; AWWA, 2018). The bulk density of the RDLP of 0.34 $g\ mL^{-1}$ was deemed suitable as it was higher than the lower limit of bulk density (0.25 $g\ mL^{-1}$) according to the American Water Works Association (AWWA) standard (Bouamama, 2017; AWWA,1991). Higher bulk density ensures improved packing and enhanced filtration efficiency of the adsorbent. This combined low moisture, low ash content, and suitable bulk density indicates the potential applicability of RDLP for adsorption from aqueous solutions. RDLP exhibited a slightly acidic pH of 6.5, which is favourable for the adsorption of divalent ions (Ridha *et al*., 2020; Ekere *et al*.,2015).The electrical conductivity (118 µS/cm) of the RDLP suggests limited leachable impurities and good stability of the adsorbent (Campisi *et al*., 2018; Horsfall *et al*., 2012).

The scanning electron micrograph of RDLP (Figure 1) reveals uneven, rough, and porous surface structures, which are a requirement for a potential adsorbent.

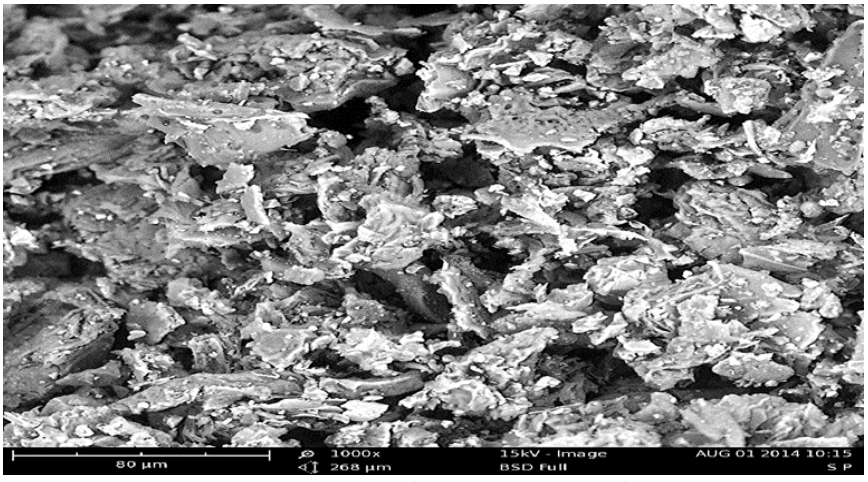

Figure 1: Scanning Electron Micrograph of *Rinorea dentata* Leaf Powder (RDLP)

The energy-dispersive X-ray spectrum shows that the adsorbent is predominantly made of carbon, as presented in Figure 2 and Table 3. It should be noted that the relatively high carbon signal (65.8%) detected by EDX is characteristic of untreated lignocellulosic biomass, which is rich in cellulose, hemicellulose, and lignin. These structural polymers naturally contribute to a carbon-dominated surface composition (Zhang *et al.,* 2023). The presence of oxygen (13.4 %) and nitrogen (9.8 %) indicates the presence of oxygenated and nitrogen functionalities, which could enhance the adsorption properties of the biomass.

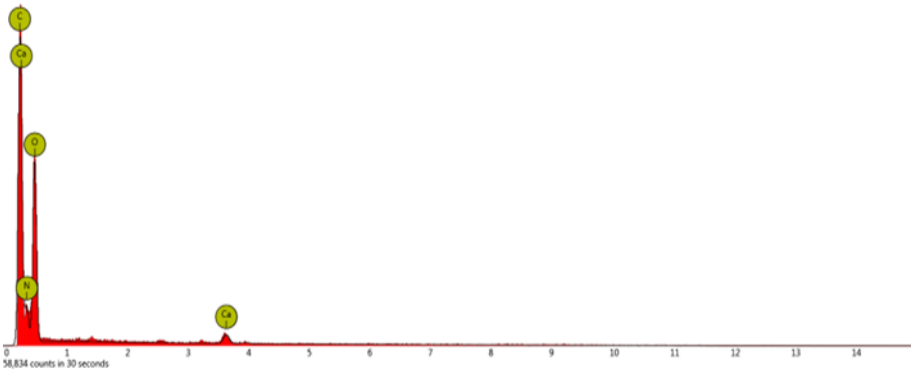

Figure 2: Energy Dispersive X-ray Spectrum of RDLP

The notable presence of calcium (0.9 %), though in small quantities, may naturally exist as part of the plant structure, and could also provide some benefit for metals' adsorption applications, conferring probable ion exchange sites for adsorbate metal ions.

Table 2: Elemental Composition of RDLP

Element Number	Element Symbol	Element Name	Concentration	Error
6	C	Carbon	65.8	1.0
20	Ca	Calcium	0.9	0.4
8	O	Oxygen	13.4	0.8
7	N	Nitrogen	9.8	2.3

Effect of Solution pH

Figure 3 shows the effect of solution pH on the removal of Pb^{2+} and Cd^{2+} ions by the RDLP adsorbent. The adsorption efficiency increased with increasing pH and reached a maximum at pH 6.0, which was therefore selected as the optimum pH for all subsequent experiments. Several reports indicated a pH of 5–6 as optimum for the adsorption of metals such as Pb^{2+}, Cu^{2+}, $Mn^{2+,}$ and Zn^{2+} from aqueous solutions (Singh, 2024; Chang *et al*., 2023; El-Sayed & El-Sayed, 2022; Kumar & Singh, 2021). At lower pH values, there was a corresponding decrease in the % removal of the metal ions. At strongly acidic conditions (low pH), excess H^{+} ions compete with Pb^{2+} and Cd^{2+} for available adsorption sites on the RDLP surface, leading to reduced metal uptake. In addition, the adsorbent surface becomes more protonated under acidic conditions, which limits electrostatic attraction between the positively charged metal ions and the adsorption sites. At higher pH values, the formation of hydroxylated complexes of the metal ions may occur, which can compete with active adsorption sites, thereby decreasing the retention of metal ions on the adsorbent (Faith *et al*., 2021; Lee & Park, 2018).

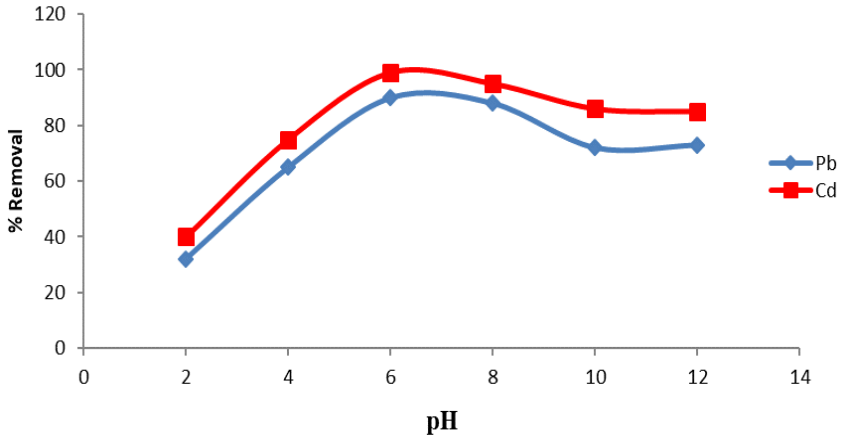

Figure 3: The Effect of pH on the Percentage Removal of Pb^{2+} and Cd^{2+}ions from Aqueous Solution onto RDLP

Effect of Initial Metal ion Concentrations

The metal ion uptake rate of RDLP is a function of the initial metal ion concentration, making it a vital factor to be examined for an excellent sorption experiment. Figure 4 illustrates the effect of initial metal ion concentration on the adsorption of Pb^{2+} and Cd^{2+} by RDLP. Percentage removal for both ions decreased with increasing metal ion concentration, and this is attributed to saturation of available adsorption sites at higher concentrations. At lower concentrations, sufficient active sites are available relative to the number of metal ions, resulting in higher removal efficiencies (Li et *al*., 2022). Pb^{2+} ions exhibited higher removal efficiency than Cd^{2+} ions at comparable concentrations, likely due to differences in ionic radius and affinity for surface functional groups.

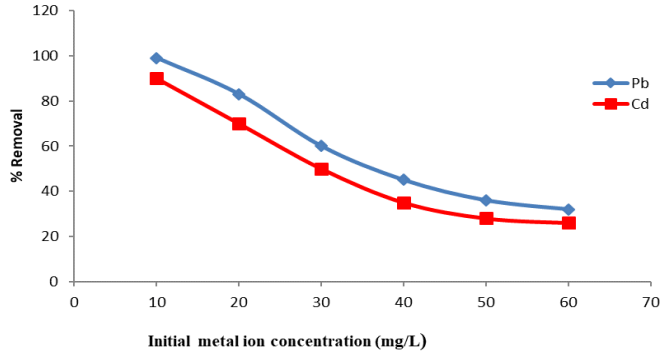

Figure 4: The Effect of Initial Metal Ions Concentration on the Percentage Removal of Pb^{2+} and Cd^{2+} ions from Aqueous Solution onto RDLP

Effect of Contact Time

The influence of contact time on the percentage removal of Pb^{2+} and Cd^{2+} was investigated at different contact times (20 to 120 minutes) and is represented in Figure 5. Adsorption was rapid initially and then slowed down until equilibrium was attained at approximately 80 minutes. The slower uptake of the metal ions in the later stages could be due to saturation of the attachment-controlled process caused by less available active sites for adsorption, while there was a gradual decrease in percentage removal with increase in contact time from 100 to 120 minutes reflects saturation of the active surface sites of the adsorbent with the metal ions which reduces the driving force for mass transfer (Li *et al.*, 2022; Wu *et al.*, 2020).

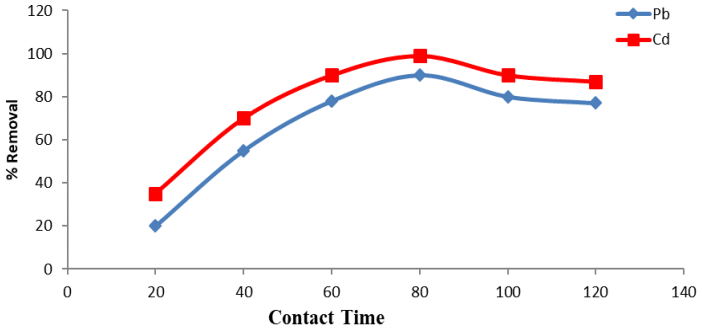

Figure 5: Effect of Contact Time on the Percentage Removal of Pb^{2+} and Cd^{2+} ions from Aqueous Solution onto RDLP

Effect of Adsorbent Dosage

As shown in Figure 6, there was a corresponding increase in the percentage removal of Pb^{2+} and Cd^{2+} with an increase in the adsorbent dose of RDLP from 0.1 to 0.6 g. This corresponding increase was due to an increase in the sorptive surface area and the availability of more active binding sites on the surface of the RDLP with increase in adsorbent dose (Li *et al.*, 2022; Wu *et al.*, 2020; Ekere *et al.*, 2015). However, beyond a certain dosage, adsorption capacity per unit mass may decrease due to particle aggregation and site overlap.

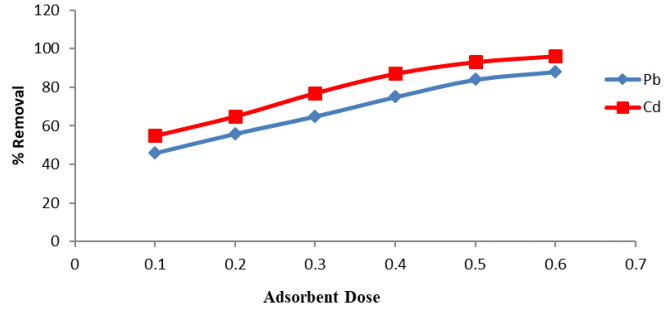

Figure 6: Effect of Adsorbent Dose on the Percentage Removal of Pb^{2+} and Cd^{2+} ions from Aqueous Solution onto RDLP

Effect of Particle Size

The influence of varying the RDLP particle size on the adsorption of Pb^{2+} and Cd^{2+} onto the adsorbent is shown in Figure 7. A decrease in the percentage removal of the metal ions was observed with increasing particle size. This could be due to the increase in the total surface area, which provided more active sites for adsorption of the metal ions at smaller particle sizes (Ekere *et al.*, 2015) as well as shorter diffusion paths. Smaller particles help to provide more active sites on the surface of the adsorbent, resulting in more accessibility for metal ions due to better diffusion. The reduced efficiency at larger particle sizes is due to decreased surface area and limited accessibility of active sites (Li *et al.*, 2022).

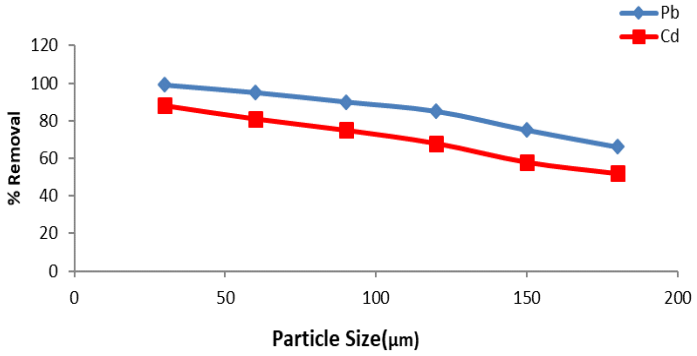

Figure 7: Effect of Particle Size on the Percentage Removal of Pb^{2+} and Cd^{2+} ions from Aqueous Solution onto RDLP

Effect of Temperature

Figure 8, shows the effect of solution temperature on the adsorption of Pb^{2+} and Cd^{2+} ions onto RDLP adsorbent. There was an increase in adsorption of Pb^{2+} and Cd^{2+} ions with an increase in solution temperature from 300 to 350 K, as shown from the graph. The increase in the percentage removal of the metal ions at higher temperatures may be due to greater kinetic energy acquired by the metal ions with an increase in solution temperature, which enhances the diffusion from the bulk solution onto the surface of RDLP (Li *et al.*, 2022; Wu *et al.*, 2020).

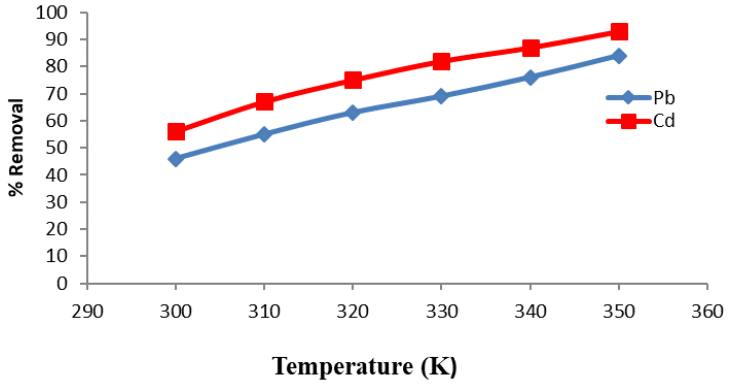

Figure 8 Effect of Solution Temperature on the Percentage Removal of Pb^{2+} and Cd^{2+} ions from Aqueous Solution onto RDLP

Adsorption Isotherm

The parameters of equilibrium isotherms give useful information on the sorption mechanism, surface properties, and affinity of the adsorbent for the adsorbate (Wu *et al*., 2020; Wang & Guo, 2020). Therefore, it is very crucial to ascertain the most suitable isotherm model to maximize the status for designing adsorption systems. This study utilized the Langmuir and the Freundlich isotherms to analyze the equilibrium data, and the results are presented in Table 3. The Langmuir isotherm is normally used to describe adsorption patterns, which is based on the assumption that the uptake of metal ions occurs on a homogenous surface by monolayer sorption without interaction between the adsorbed molecules (Bayuo*et al*., 2018; Ekere *et al.*, 2015). The linear form of the Langmuir isotherm equation is expressed as:

$$\frac{C_e}{q_e} = \frac{1}{K_a q_{max}} + \frac{C_e}{q_{max}}. \qquad (3)$$

where C_e = the metal ion concentration in the solution at equilibrium (mg/L); q_e = the monolayer adsorption capacity of the adsorbent (mg/g); K_a = the Langmuir adsorption constant (L/mg) which is related to the adsorption energy, and quantitatively reflects the affinity between the adsorbent and the adsorbate; q_{max} = the maximum monolayer adsorption capacity of adsorbent (mg/g). While the constant, q_{max} and K_a can be determined from the slope and the intercept of the linear plot of $\frac{C_e}{q_e}$ against C_e as shown in Figures 9 and 10 below. The most important features of the Langmuir isotherm is expressed in terms of a dimensionless constant, the separation factor (R_L) which is defined by the relationship given in equation 4:

$$R_L = \frac{1}{[1 + K_{aC_o}]} \qquad (4)$$

C_o = the initial metal ions concentration (mg/L) and $K_a$is the Langmuir equilibrium constant (L/mg). The value of the separation factor provides important information about the nature of the adsorption process. The adsorption is said to be irreversible (R_L = 0), favourable (0 <R_L<1), linear (R_L= 1), or unfavourable (R_L>1) (Folasegun & Kovo, 2014; Foo & Hameed, 2010). From Table 3, the correlation coefficient (R^2) for the Langmuir isotherm indicated a good fit for the adsorption of Pb^{2+} and Cd^{2+} ions onto RDLP.

The Freundlich isotherm model is applied to describe the amount of substance adsorbed per unit gram of the adsorbent (q_e) and is related to the equilibrium concentration (C_e) of the metal ions, and the linear form of the equation is given as:

$$\log q_e = \frac{1}{n}\log C_e + \log K_f \qquad (5)$$

Where K_f = the constant indicative of the relative adsorption capacity of the adsorbent (mg/g)

n = the constant indicative of the intensity of the adsorption

The constants were determined by the linear plot of $\log q_e$ versus $\log C_e$ as shown in Figures 11 and 12. In the Freundlich

isotherm model, if the value of n lies between 1 and 10, it indicates favorable adsorption.

In this study, the value of n obtained for the adsorption of Pb^{2+} and Cd^{2+} by RDLP was in the range of 5.952 to 8.696, indicating a favorable adsorption process. However, the relatively low q_{max} values (1.634 mg/g for Pb^{2+} and 1.263 mg/g for Cd^{2+}) reflect the absence of chemical activation of RDLP and its low pore volume.

Table 3: Langmuir and Freundlich Isotherm Constants for the Adsorption of Pb^{2+} and Cd^{2+}ions onto RDLP

	Langmuir model			Freundlich model		
Metal ions	**q_{max} (mg/g)**	**K_a (L/mg)**	**R^2**	**K_f (mg/g) (mg/L)$^{1/n}$**	**n**	**R^2**
Pb^{2+}	1.634	2.125	0.980	1.028	5.952	0.905
Cd^{2+}	1.263	1.189	0.992	1.164	8.696	0.958

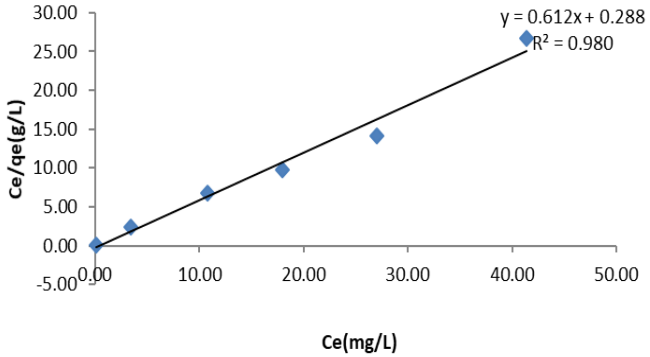

Figure 9: Langmuir Adsorption Isotherm for Pb^{2+}Ion by RDLP

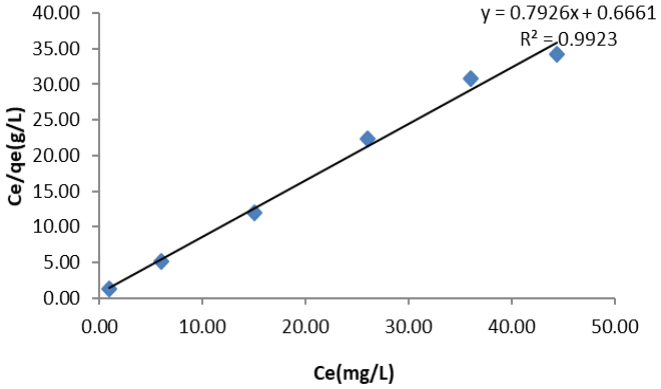

Figure 10: Langmuir Adsorption Isotherm for Cd^{2+} ion by RDLP

The Freundlich and Langmuir isotherm models indicated a good fit to the adsorption experimental data, having values closer to 1(Figs. 9 -12). The reasonable agreement of both Langmuir and Freundlich isotherm models suggests that adsorption occurred on a heterogeneous surface with favorable interaction between RDLP and metal ions (Kajjumba *et al*., 2019).

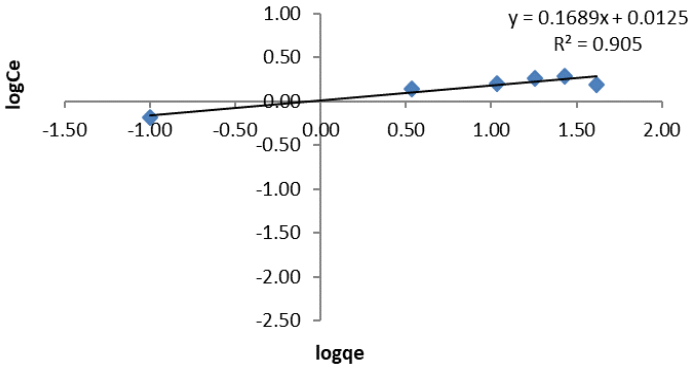

Figure 11: Freundlich Adsorption Isotherm for Pb^{2+} Ion by RDLP

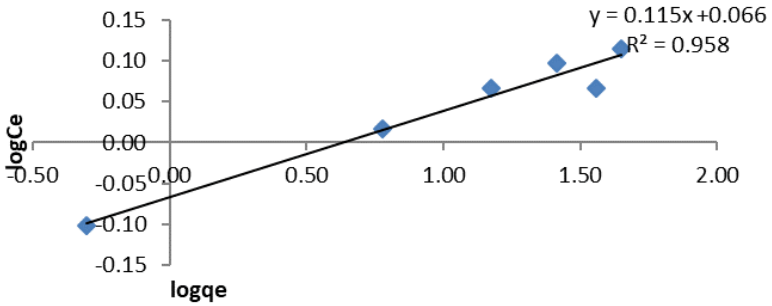

Figure 12: Freundlich Adsorption Isotherm for Cd^{2+} ion by RDLP

Table 4: Langmuir Equilibrium Parameter (R_L) Ranges for Adsorption of Pb^{2+} and Cd^{2+} Ions onto RDLP

METAL IONS	Range of RL VALUES
Pb2+	0.0449 – 0.0075
Cd2+	0.0776 – 0.0138

The range of R_L values at different initial adsorbate concentrations (10, 20, 30, 40, 50, and 60 mg/L) for Pb^{2+} and Cd^{2+} ions (Table 4) indicated a favorable adsorption process of the metals onto RDLP having R_L values < 1.

Adsorption Kinetics

The pseudo-first order, pseudo-second order, and intraparticle diffusion kinetic models were fitted to the experimental data to analyze the adsorption rate and the possible adsorption mechanism of the metal ions onto RDLP. The results are shown in Table 5.

The pseudo-first order kinetic model also known as the Lagergren equation is expressed as:

$$\log(q_e - q_t) = \log q_e - (\frac{K_1}{2.303})t \quad (6)$$

Where q_t and q_e are the amount of metal ions adsorbed at time t and equilibrium in mg/g, respectively. K_1 is the pseudo-first order adsorption rate constant (min^{-1}), while the slope and intercept of the plots of $\log(q_e - q_t)$ versus t were used to determine the rate constant (K_1) and q_e, as shown in Figure 13, and the values are recorded in Table 5.

Table 5: Kinetic Model Parameters for the Adsorption of Pb^{2+} and Cd^{2+} ions from Aqueous Solutions onto RDLP

	Pseudo-first order			Pseudo-second order				Intraparticle diffusion		
Metal ions	$q_e$cal (mg/g)	k_1(min^{-1})	R^2	h (mg/gmin)	k_2 (g/mgmin)	q_{ecal} (mg/g)	R^2	k_{id} (mg/gmin)	I	R^2
Pb^{2+}	1.242	0.00921	0.954	0.0228	0.00973	1.531	0.779	0.113	1.114	0.886
Cd^{2+}	2.138	0.023	0.972	0.0256	0.00394	2.551	0.462	0.216	0.449	0.980

The Pseudo-First-Order Equation Provided the Best Fit to the Experimental Data for Pb^{2+} and Cd^{2+} ions Adsorbed by RDLP Having Regression (R^2) Values Closer to 1.

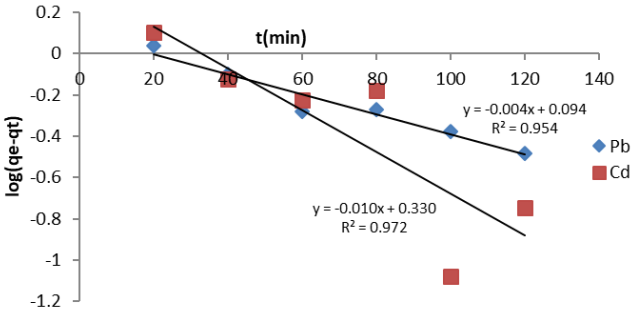

Figure 13: Pseudo-First Order Adsorption Kinetic for Pb^{2+} and Cd^{2+} Ions by RDLP

The pseudo-second-order kinetic model is based on the assumption that chemisorption is the rate-determining step and is given as:

$$\frac{t}{q_t} = \frac{1}{K_2 q_e^2} + \left(\frac{1}{q_e}\right)t \quad (7)$$

$$\frac{t}{q_t} = \frac{1}{h} + \left(\frac{1}{q_e}\right)t \quad (8)$$

where t = contact time (min), q_t and q_e are the amount of metal ions adsorbed at time and equilibrium in (mg/g), K_2 is the equilibrium rate constant of pseudo-second order adsorption (g/mg min). The values of q_e and K_2 were calculated from the slope and intercept of the linear plot of t/q_t versus t as shown in Figure 14. The initial sorption rate, h (mg/g min), was calculated from the equation:

$$h = K_2 q_e^2 \quad (9)$$

The pseudo-second order equation did not provide a good fit to the experimental data for Pb^{2+} and Cd^{2+} ions, having regression coefficient (R^2) values (0.462 - 0.779), This suggests that the adsorption process may be predominantly governed by physical interactions rather than chemisorption, although the pseudo-second order model has been found to

provide the best fit to most adsorption studies (Foo & Hameed, 2010). The better fit provided by the pseudo-first order model suggests that the adsorption mechanism is predominantly governed by physisorption involving weak van der Waals forces, rather than any form of chemical interactions (Weber & Morris, 1963).

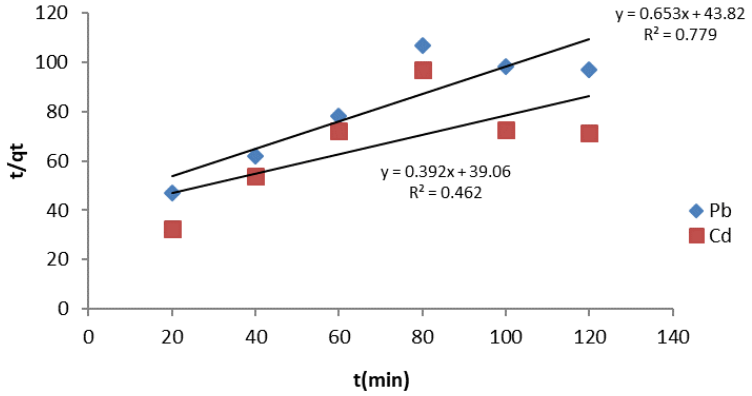

Figure 14: Pseudo-Second Order Adsorption Kinetics for Pb^{2+} and Cd^{2+} ions by RDLP

The kinetic data were also analyzed using Weber and Morris's intraparticle diffusion model to elucidate the diffusion mechanism. The initial rate of the intraparticle diffusion is expressed as:

$$q_t = K_{id}\, t^{1/2} + I \qquad (10)$$

where K_{id} is the intraparticle diffusion rate constant ($mg/gmin^{1/2}$), and l is the intercept. The intercept of the plot indicated the boundary layer effect. The constant K_{id} was obtained from the slope of the plot of q_t versus $t^{1/2}$ as shown in Figure 15. Intraparticle diffusion is the sole rate-determining step if the plot is linear and passes through the origin (Foo & Hammed, 2010).

In Table 5, the regression coefficient (R^2) value for Cd^{2+} ions was close to 1. The presence of the intercept (I) shows the existence of the surface sorption, indicating that intraparticle diffusion was not the only rate-limiting step (Foo & Hammed, 2010). The non-zero intercept of the Weber- Morris plot revealed that intraparticle diffusion was not the sole rate - limiting step, indicating that surface adsorption and boundary layer effects played a significant role.

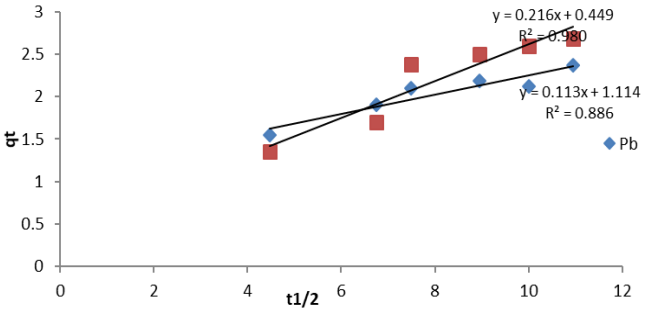

Figure 15: Intraparticle Diffusion Model for Pb^{2+} and Cd^{2+} ions Biosorption onto RDLP

Thermodynamic Considerations

The free energy change (ΔG^o), enthalpy change (ΔH^o), and entropy change (ΔS^o) thermodynamic parameters were determined to evaluate the feasibility of the adsorption process of Pb^{2+} and Cd^{2+} ions onto RDLP. The thermodynamic feasibility of the adsorption process was assessed using the temperature dependence of the apparent equilibrium constant (Kc) in the temperature range of 300–350 K.

The Gibbs free energy change of the adsorption was calculated using the equation below:

$$\Delta G^o = -RT \ln K_c \qquad (11)$$

where T is the temperature (K); R is the universal gas constant (8.314 J/mol K) and Kc is the apparent equilibrium constant obtained from the adsorption data.

The values of $\Delta G°$ calculated at different temperatures were negative for both Pb^{2+} and Cd^{2+} ions (Table 6), indicating that the adsorption process is thermodynamically favourable. It was also observed that the magnitude of $\Delta G°$ increased with an increase in temperature, becoming more negative at higher temperatures, suggesting that adsorption was more favourable at elevated temperatures.

Table 6: Thermodynamic Parameters for the Adsorption of Pb^{2+} and Cd^{2+} Ions from Aqueous Solution onto RDLP

Metal ion	T (K)	K_c	ΔG^o (kJ/mol)	ΔH^o (kJ/mol)	ΔS^o (J/mol K)	R^2
Pb^{2+}	300	1.27	−0.596	14.321	49.866	0.996
	310	1.56	−1.146			
	320	1.86	−1.651			
	330	2.23	−2.200			

Metal ion	T (K)	K_c	ΔG^o (kJ/mol)	ΔH^o (kJ/mol)	ΔS^o (J/mol K)	R^2
	340	2.57	−2.668			
	350	2.85	−3.048			
Cd^{2+}	300	1.85	−1.534	15.026	54.931	0.991
	310	2.13	−1.949			
	320	2.56	−2.501			
	330	3.00	−3.014			
	340	3.76	−3.744			
	350	4.26	−4.217			

The enthalpy change (ΔH^o) and entropy change (ΔS^o) of the adsorption process were determined using the Van't Hoff equation as shown below:

$$InK_c = -\left(\frac{\Delta H^o}{RT}\right) + \left(\frac{\Delta S^o}{R}\right) \quad (12)$$

The values of enthalpy change (ΔH^o) and entropy change (ΔS^o) were calculated from the slope and intercept of the plot of lnKc against 1/T as shown in Figure 16. The positive values of enthalpy change obtained for Pb^{2+} (14.321 kJ/mol) and Cd^{2+} (15.026 kJ/mol) ions indicate that the adsorption process is endothermic in nature. The relatively low magnitude of ΔH° values (< 20 kJ/mol) suggests that the adsorption of the metal ions onto RDLP is predominantly governed by physical interactions rather than chemical bonding. Physisorption typically ranges between 2–20 kJ/mol,whereas chemisorption is generally reported in the range of 80–200 kJ/mol (Foo & Hameed, 2010).Thepositive ΔS^o values show an increase in randomness at the solid/liquid interface during the adsorption process (Kajjumba *et al*., 2019; Weber & Morris,1963).

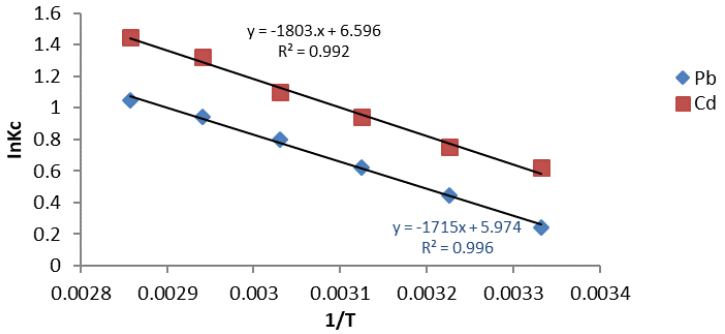

Figure 16: Thermodynamic Adsorption for Pb^{2+} and Cd^{2+} ions by RDLP

This increase in disorder may be attributed to the displacement of water molecules surrounding the hydrated metal ions as adsorption proceeds on the RDLP surface. The reaction is spontaneous as negative values of ΔG^o were obtained at all the temperatures studied. Overall, the thermodynamic parameters indicate that the adsorption of Pb^{2+} and Cd^{2+} ions onto RDLP is feasible, endothermic and spontaneous in nature.

CONCLUSION

This study has demonstrated the potential of the *Rinorea dentata* leaf powder (RDLP) as a low-cost adsorbent for Pb^{2+} and Cd^{2+} ions sequestration from aqueous solutions. The findings indicated that the percentage removal of RDLP for both metal ions was considerably influenced by solution pH, initial metal ion concentration, contact time, adsorbent dosage, size of the adsorbent particles, and solution temperature. Optimum adsorption was obtained at pH 6, 0.6 g adsorbent dosage, 80 min contact time, and smaller particle size under ambient experimental conditions. The equilibrium adsorption data were well described by both the Langmuir and the Freundlich isotherm models, depicting a favourable adsorption process onto a heterogeneous adsorbent surface. The pseudo-first-order kinetics model aligned most closely with the kinetic data, as evidenced by higher correlation coefficient (R^2) values compared to the pseudo-second-order model, suggesting a physisorption-dominated adsorption mechanism, with intraparticle diffusion contributing to the overall rate but not serving as the sole rate-controlling step. The adsorption was confirmed to be feasible and endothermic in nature. The use of this adsorbent, which is inexpensive, easily accessible, and eco-friendly, makes its use economical compared to chemically activated adsorbents, thus making it a promising material for preliminary sequestration of Pb^{2+} and Cd^{2+} ions from aqueous contaminated water. Furthermore, the abundance, low cost, and minimal processing requirements of RDLP highlight its strong potential for scale-up and application in industrial wastewater treatment systems**.** It is recommended that further studies be undertaken to elucidate its practical applicability by exploring its regeneration, reusability, and performance in real water systems

Statements and Declarations

Competing Interest

The authors have declared that they have no competing interests.

Funding

There were no specific funds provided to the authors for this work.

REFERENCES

Abiodun, O. A. O., Oluwaseun, O., Oladayo, O. K., Abayomi, O., George, A. A., Opatola, E., Orah, F. R., Isukuru, J.E., Ede, C. I., Oluwayomi, O. T., Okolie, J. A., & Omotayo, I. A. (2023). Remediation of heavy metals using biomass-based adsorbents: Adsorption kinetics and isotherm models. *Clean Technologies*, *5*, 934–960. Doi: https://doi.org/10.3390/cleantechnol5030047

Alexander, B., Evgeny, V. G., Irina, V. B., Anastassia, E. K., Shilpi, A., Alexey, G. T., & Vinod, K. G. (2018). Adsorption

of heavy metals on conventional and nanostructured materials for wastewater treatment purposes: A review. *Ecotoxicology and Environmental Safety, 148,* 702–712. Doi: https://doi.org/10.1016/j.ecoenv.2017.11.034

Aliyu A. U., Musa, S., Garba, H., Ahmad, S., & Hausa, S. S. K. (2026). Isolation and evaluation of indigenous fungal species for biosorption of cadmium (Cd) from contaminated soil. *FUDMA Journal of Sciences, 10*(6), 69–73. Doi: https://doi.org/10.33003/fjs-2026-1006-5070

American Water Works Association. (1991). *AWWA standards for granular activated carbons*. AWWA.

American Water Works Association. (2018). *Activated carbon adsorption for water treatment* (3rd ed.). AWWA.

Ansam, Q. J., & Sata, K. A. (2024). Removal of heavy metal ions from wastewater using ion-exchange resin in a batch process: Kinetic and isotherm studies. *South African Journal of Chemical Engineering, 49,* 43–54. Doi: https://doi.org/10.1016/j.sajce.2024.04.002

Anwar, H. S., Noorfidza, Y. H., & Neisha, Z. (2020). Heavy metals capture from water sludge by kenaf fibre activated carbon in batch adsorption. *Journal of Ecological Engineering, 21,* 102–115. Doi: https://doi.org/10.12911/22998993

ASTM International. (2015). *ASTM D7582–15: Standard test methods for proximate analysis of coal and coke by macro thermogravimetric analysis*. ASTM International. Doi: https://www.astm.org/d7582-15.html

Attah, F., Hellinger, R., Sonibare, A. M., Moody, O. J., Arrowsmith, S., Wray, S., & Gruber, W. C. (2016). Ethnobotanical survey of Rinorea dentata (Violaceae) used in South-Western Nigerian ethnomedicine and detection of cyclotides. *Journal of Ethnopharmacology, 179*, 83–91. Doi: https://doi.org/10.1016/j.jep.2015.12.038

Bayuo, J., Pelig-Ba, K., &Abukari, M. (2018). Isotherm modeling of lead (II) adsorption from aqueous solution using groundnut shell as a low-cost adsorbent. *IOSR Journal of Applied Chemistry, 11*(1), 18–23. Doi: https://doi.org/10.9790/5736-1111011823

Bayuo, J., Rwiza, M. J., Choi, J. W., Mtei, K. M., Hosseini-Bandegharaei, A., & Sillanpää, M. (2024). Adsorption and desorption processes of toxic heavy metals, regeneration and reusability of spent adsorbents: Economic and environmental sustainability approach. *Advances in colloid and interface science, 329,* 103196. Doi: https://doi.org/10.1016/j.cis.2024.103196

Bouamama, A., Abdellah, A., Stéphane, M., Anne, P., Nasre-Dine, A., Laurent, B., & Davy, D. (2017). Removal of Cu^{2+}, Pb^{2+}, and Zn^{2+} by flax fibres. *Process Safety and Environmental Protection, 109,* 639–647. Doi: https://doi.org/10.1016/j.psep.2017.05.012

Campisi, S., Chan-Thaw, C. E., & Villa, A. (2018). Heteroatom-mediated metal–support interactions in functionalized carbons. *Applied Sciences, 8,* 1159. Doi: https://doi.org/10.3390/app8071159

Chang, Y., Wang, H., & Li, Z. (2023). Adsorption of Cr^{6+}, Cu^{2+}, Pb^{2+}, and Zn^{2+} by magnetic nano-chitosan. *Molecules, 28*, 2607. Doi: https://doi.org/10.3390/molecules28062607

Ekere, R. N., Agwogie, B. A., &Ihedioha, N. J. (2015). Biosorption of Pb^{2+}, Cd^{2+} and Cu^{2+} from aqueous solutions using Adansonia digitata root powder. *International Journal of Phytoremediation, 18,* 116–125. Doi: https://doi.org/10.1080/15226514.2015.1058329

El-Sayed, E. M., & El-Sayed, Z. A. (2022). Removal of Cu(II), Pb(II), and Zn(II) using agricultural wastes. *Journal of Water Resource and Protection, 14,* 123–135. Doi: https://doi.org/10.4236/jwarp.2022.143008

Faith, C., Njenga, M., & Beatrice, K. (2021). Adsorption of Pb, Cu, and Zn in multi-metal systems using waste rubber tires. *Heliyon, 7,* e08254. Doi: https://doi.org/10.1016/j.heliyon.2021.e08254

Fajobi M.O., Lasode O.A., Adeleke, A.A., Ikubanni, P.P., Balogun, A.O. (2022) Investigation of physicochemical characteristics of selected lignocellulose biomass. Sci Rep. 2022 Feb 21;12(1):2918. Doi: https://doi.org/10.1038/s41598-022-07061-2

Folasegun, D. A., &Kovo, A. S. (2014). Simultaneous adsorption of Ni(II) and Mn(II) from aqueous solution using rice husk ash. *Journal of Materials Research and Technology, 3*(2), 129–141. Doi: https://doi.org/10.1016/j.jmrt.2014.03.002

Foo, Y. K., & Hameed, H. B. (2010). Insights into adsorption isotherm modeling. *Chemical Engineering Journal, 156*, 2–10. Doi: https://doi.org/10.1016/j.cej.2009.09.013

Haerdi, F. (1964). Rinorea species records. *JSTOR Global Plants.* https://plants.jstor.org/stable/history/10.5555/al.ap.upwta.5_514

He, J., & Chen, J. P. (2014). A comprehensive review on biosorption of heavy metals by algal biomass: Materials, performances, chemistry, and modeling simulation tools. *Bioresource Technology, 160,* 67–78. Doi: https://doi.org/10.1016/j.biortech.2014.01.068

Horsfall Jnr, M., Verla, E. N., Spiff, I. A., &Ekpete, O. A. (2012). Preparation and characterization of activated carbon from fluted pumpkin (*Telfairia occidentalis*Hook.f) seed shell. *Research Journal of Chemical Sciences, 2*(10), 10–15. Doi: https://doi.org/10.13140/RG.2.2.30627.04647

Jain, K. C., Malik, S. D., & Yadav, K. A. (2016). Applicability of plant-based biosorbents in heavy-metalremoval: A review. *Environmental Processes, 3,* 495–523. Doi: https://doi.org/10.1007/s40710-016-0143-5

Jasper, E. E., Onwuka, J. C., &Bidam, M. Y. (2021). Screening of factors that influence the preparation of Dialiumguineense pods active carbon for use in methylene blue adsorption: A full factorial experimental design. *Bulletin of the National Research Centre, 45,* 168. Doi: https://doi.org/10.1186/s42269-021-00629-4

Kajjumba, G. W., Emik, S., Öngen, A., Kurtuluş Özcan, H., & Aydın, S. (2019). Modelling of adsorption kinetic

processes—Errors, theory and application. In *Advanced sorption process applications*. IntechOpen. Doi: https://doi.org/10.5772/intechopen.80495

Khulbe, C. K., & Matsuura, T. (2018). Removal of heavy metals and pollutants by membrane adsorption techniques. *Applied Water Science*, *8*, 19. Doi: https://doi.org/10.1007/s13201-018-0661-6

Kumar, A., & Singh, R. (2021). Adsorptive removal of Pb(II) and Zn(II) onto manganese oxide-coated sand. *Environmental Science and Pollution Research*, *28*, 12345–12356. Doi: https://doi.org/10.1007/s11356-020-12345-6

Kyriakopoulos, L. G., Tsimnadis, K., Sebos, I., &Charabi, Y. (2024). Effect of pore size distribution on adsorption behaviour of carbonaceous materials. *Crystals*, *14*, 742. Doi: https://doi.org/10.3390/cryst14080742

Latiza, J. P., Mustafa, A., Delos Reyes, K., Nebres, L. K., & Rubi, V. C. R. (2024). Adsorbents derived from plant sources: Current research and future outlook. *Engineering Proceedings*, *67*, 15. Doi: https://doi.org/10.3390/engproc2024067015

Lee, H. J., & Park, J. (2018). Adsorption of Pb^{2+} and Zn^{2+} using Opuntia powder. *Desalination and Water Treatment*, *135*, 330–340. Doi: https://doi.org/10.5004/dwt.2018.22309

Li, J., Dong, X., Liu, X., Xu, X., Duan, W., Park, J., Gao, L., & Lu, Y. (2022). Comparative adsorption characteristics of heavy metals. *Sustainability*, *14*(23), 15579. Doi: https://doi.org/10.3390/su142315579

López Pastor, R., Pinna-Hernández, G. M., Sánchez Molina, A. J., &Acién Fernández, G. F. (2024). Influence of moisture and ash content on adsorption processes. *Heliyon*, *11*(1), e40346. Doi: https://doi.org/10.1016/j.heliyon.2024.e40346

Marzeddu, S., Décima, A. M., Camilli, L., Bracciale, P. M., Genova, V., Paglia, L., Marra, F., Damizia, M., Stoller, M., Chiavola, A., & Boni, R. M. (2022). Physical-chemical characterization of carbon-based sorbents. *Materials*, *15*, 7162. Doi: https://doi.org/10.3390/ma15207162

Mashael, A. A., & Mohammad, A. A. (2021). Nanoadsorption mechanisms of crystal violet using nano-hazelnut shell. *Journal of Water Process Engineering*, *44*, 102354. Doi: https://doi.org/10.1016/j.jwpe.2021.102354

Munvera, A. M., Ouahouo, B. M. W., Mkounga, P., Mbekou, M. I. K., Nuzhat, S., Choudhary, M. I., & Nkengfack, A. E. (2020). Chemical constituents from leaves and trunk bark of *Rinorea oblongifolia* (Violaceae). *Natural Product Research*, *34*(14), 2014–2021. Doi: https://doi.org/10.1080/14786419.2019.1573230

Nhuchhen, D. R. (2016). Prediction of carbon, hydrogen, and oxygen compositions of raw and torrefied biomass using proximate analysis. *Fuel*, *180*, 348–356. Doi: https://doi.org/10.1016/j.fuel.2016.04.058

Pohl, A. (2020). Removal of heavy metal ions from water and wastewaters by sulfur-containing precipitation agents. *Water, Air, & Soil Pollution*, *231*, 503. Doi: https://doi.org/10.1007/s11270-020-04863-w

Ridha, A.-S. N., Kamal, M. N., & Ridha, A.-S. M. (2020). Effect of adsorption on electrical conductivity and ionization constants. *Journal of Physics: Conference Series*, *1660*, 012021. Doi: https://doi.org/10.1088/1742-6596/1660/1/012021

Saikat, M., Arka, J. C., Abu, M. T., Talha, B. E., Firzan, N., Ameer, K., Abubakr, M. I., Mayeen, U. K., Hamid, O., Fahad, A. A., & Jesus, S.-G. (2022). Impact of heavy metals on the environment and human health: Novel therapeutic insights to counter toxicity. *Journal of King Saud University – Science*, *34*, 101865. Doi: https://doi.org/10.1016/j.jksus.2022.101865

Saleem, J., Shahid, U., Hijab, M., Hamish, M., & Gordon, M. (2019). Production and applications of activated carbons from olive stones. *Biomass Conversion and Biorefinery*, *9*, 775–802. Doi: https://doi.org/10.1007/s13399-019-00473-7

Shankar, P., Thandapani, G., Kumar, V., & Sudha, P. N. (2022). Evaluation of batch and packed-bed adsorption columns for chromium(VI) ion removal using chitosan–silica–g–AM/orange peel hydrogel composite. *Biomass Conversion and Biorefinery*, *14*, 2745–2760. Doi: https://doi.org/10.1007/s13399-022-02450-z

Singh, V., Ahmed, G., & Vedika, S. (2024). Toxic heavy metal ion contamination in water and their sustainable reduction by eco-friendly methods: Isotherms, thermodynamics and kinetics study. *Scientific Reports*, *14*, 7595. Doi: https://doi.org/10.1038/s41598-024-58061-3

Sohail, A., Asif, A. S., Md., S. K., Ahmad, Z., Izhar, A., Esrafil, A., & Fazlollah, C. (2020). Removal of heavy metals (Cr, Cu, and Zn) from electroplating wastewater by electrocoagulation and adsorption processes. *Desalination and Water Treatment*, *179*, 263–271. Doi: https://doi.org/10.5004/dwt.2020.25010

Subhashish, D., Veerendra, G. T. N., Phani, M. A. V., & Anjaneya Babu, P. S. S. (2023). Performance of plant-leaf biosorbents for phosphorus removal from synthetic water. *Cleaner Materials*, *8*, 100191. Doi: https://doi.org/10.1016/j.clema.2023.100191

Usman, I. M., Muhammad, V. S., & Sagheer, O. A. (2024). Adsorptive removal of heavy metals from aqueous solutions: Progress in adsorbent development and effectiveness. *Environmental Research*, *251*, 118562. Doi: https://doi.org/10.1016/j.envres.2024.118562

Wang B, Lan J, Bo C, Gong B, Ou J(2023). Adsorption of heavy metal onto biomass-derived activated carbon: review. RSC Adv. 31;13(7):4275-4302. Doi: https://doi.org/10.1039/d2ra07911a

Wang, J., & Guo, X. (2020). Adsorption isotherm models: Classification and application. *Chemosphere*, *258*, 127279. Doi: https://doi.org/10.1016/j.chemosphere.2020.127279

Weber, W. J., & Morris, J. C. (1963). Kinetics of adsorption on carbon from solution. *Journal of the Sanitary Engineering Division*, *89*(2), 31–60. Doi: https://doi.org/10.1061/jsedai.0000430

Wu, Z., Ye, X., Liu, H., Zhang, H., Liu, Z., Guo, M., Li, Q., & Li, J. (2020). Interactions between adsorbents and adsorbates in aqueous systems. *Pure and Applied Chemistry*,

92(10), 1655–1662. Doi: https://doi.org/10.1515/pac-2019-1110

Xie, S. (2024). Biosorption of heavy metal ions from contaminated wastewater: An eco-friendly approach. *Green Chemistry Letters and Reviews*, *17*. Doi: https://doi.org/10.1080/17518253.2024.2357213

Zhang, Y., Li, X., Wang, J., & Chen, Y. (2023). Adsorption of Pb^{2+} and Zn^{2+} by magnetic biochar. *Toxics*, *11*, 590. Doi: https://doi.org/10.3390/toxics11070590

Zhou, L., Yu, Q., Cui, Y., Xie, F., Li, W., Li, Y., & Chen, M. (2017). Adsorption properties of reed-derived activated carbon. *Ecological Engineering*, *102*, 443–450. Doi: https://doi.org/10.1016/j.ecoleng.2017.02.036